

# Gas-Phase Reaction Pathways of Aluminum Organometallic Compounds with Dimethylaluminum Hydride and Alane as Model Systems

Brian G. Willis<sup>†</sup> and Klavs F. Jensen\*

Department of Chemical Engineering, Massachusetts Institute of Technology, Cambridge, Massachusetts 02139

Received: March 14, 2000; In Final Form: June 1, 2000

Gas-phase molecular association reactions of dimethylaluminum hydride have been studied with density functional theory (DFT) and ab initio MP2 methods to understand the dimer  $\rightleftharpoons$  trimer equilibrium. A mechanism involving DMAH oligomers from monomers through hexamers is proposed as the equilibrium reaction pathway, and the kinetics and thermodynamics of the mechanism have been investigated. Optimized structures, heats of reaction, and transition states have been computed for the proposed reaction pathways. For transition-state optimizations, alane oligomers  $(\text{AlH}_3)_n$  were used as model systems to simplify electronic structure calculations for quantification of the kinetics of DMAH reaction pathways. The proposed reaction pathways consist of a sequence of unimolecular and concerted bimolecular steps with activation barriers substantially less than for alternative ring-opening pathways. On the basis of the current results, experimental observations of a complex DMAH dimer  $\rightleftharpoons$  trimer equilibrium can be understood in terms of a series of these slow bimolecular and relatively faster unimolecular reactions.

## I. Introduction

Aluminum organometallic compounds, such as dimethylaluminum hydride (DMAH), are useful for the deposition of aluminum containing films with applications in semiconductor metalization and compound semiconductor devices.<sup>1–3</sup> Knowledge of the reaction pathways of these compounds is essential for understanding thin film growth and developing quantitative reactive process models. Although much is known about aluminum organometallic chemistry, there is a general lack of quality quantitative thermodynamic and kinetic data. Knowledge of thermodynamic and kinetic data along with chemical mechanisms is necessary for accurate process models. Recently, computational chemistry methods have become viable alternatives to laboratory experiments for providing physical and chemical properties of molecules.<sup>4–6</sup> For many types of compounds, these calculations generally achieve an accuracy of 3–5 kcal/mol or better for thermodynamic calculations.<sup>7</sup> Less is known regarding the accuracy of kinetic (transition state) predictions. In this paper, computational chemistry methods are employed to explore the thermodynamics and kinetics of the gas-phase molecular reaction pathways of DMAH.

While apparently simple in chemical formula  $(\text{AlH}(\text{CH}_3)_2)_2$ , DMAH is known to exist in the liquid and vapor phase as a complex equilibrium between dimers and trimers.<sup>8</sup> Observations of the liquid properties of DMAH indicate a complex viscous fluid with a time/process dependent composition.<sup>9</sup> A variable vapor phase composition is also inferred from disagreement as to the dimer/trimer composition. Early studies of DMAH indicated a dimer–trimer equilibrium over a temperature range of 80–170 °C, where trimers dominate at low temperatures and dimers predominate at higher temperatures.<sup>8</sup> In contrast, more recent studies have observed a mostly dimer concentration, even at low temperatures.<sup>10</sup> Additionally, it has been observed that the properties of the liquid differ according to the synthesis route. The complex behavior of DMAH creates challenging

issues for the use of this compound where precise control of precursor delivery rates is essential.

In this article, the approach is to relate the observed behavior of DMAH to the kinetics and thermodynamics of the molecular reaction pathways.<sup>11</sup> Interpreting the observed behavior of DMAH in terms of the thermodynamics and kinetics of elementary reaction pathways is supported by work on other aluminum organometallic compounds including the alkoxides and amides.<sup>12–14</sup> Experimental studies of these compounds have observed similar time/process dependent compositions with half-lives ranging from minutes to weeks or months depending on the compound. On the basis of studies of the above types of aluminum organometallic compounds, three basic reaction pathways have been proposed for the equilibration of dimers and trimers.<sup>15</sup>

The simplest equilibration mechanism is dissociation of dimers and trimers into monomers and subsequent recombination of monomers to form dimers or trimers.



However, breaking a dimer or trimer into monomers is highly endothermic,  $\Delta H^{298.15\text{K}} \approx +35.0$  and  $+58.5$  kcal/mol for the above DMAH reactions 1 and 2, respectively. These reactions are even more endothermic for oxygen- and nitrogen-bridged compounds, and the above mechanism is discounted by all accounts.<sup>14–16</sup>

A variation on the above pathway is ring opening of trimers and self-dissociation to form monomers and dimers.



This mechanism is partially supported by cursory evidence of monomers in experiments with amide compounds.<sup>16</sup> Note that the reverse reaction to form trimers would require the presence of monomers. This second mechanism, ring opening and self-

<sup>†</sup> Present address: 600 Mountain Ave., Murray Hill, NJ 07974.

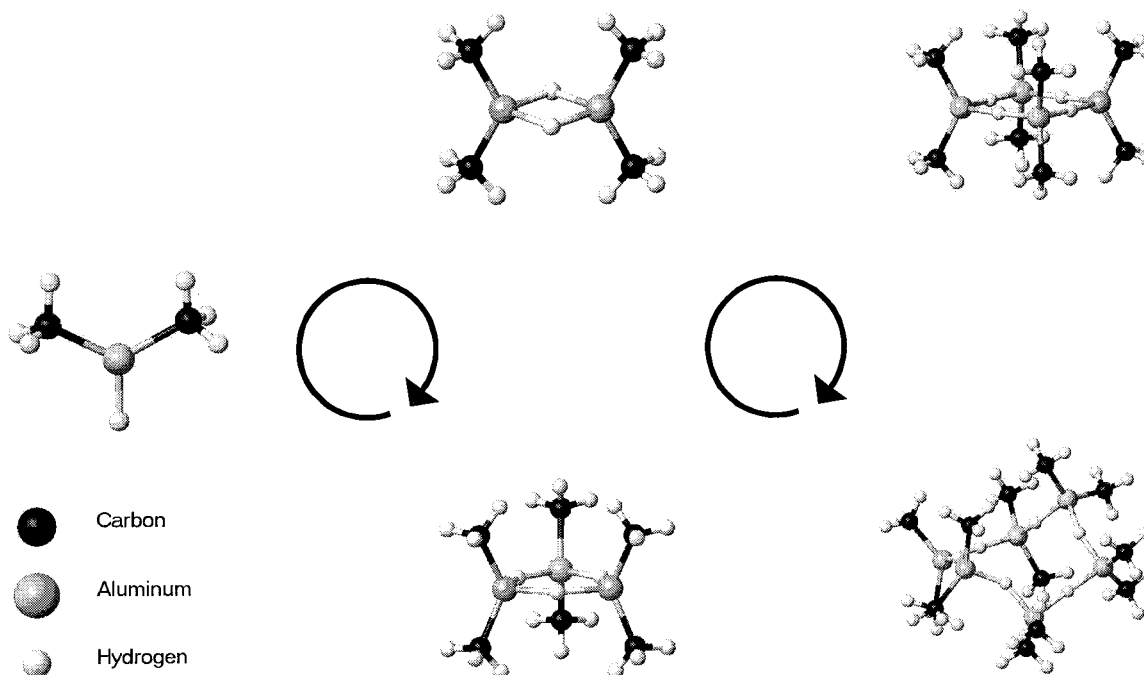
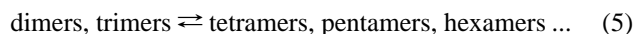
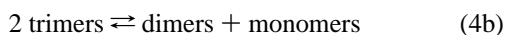


**Figure 1.** Dimethylaluminum hydride proposed reaction pathways. Clockwise from left: monomer, dimer, tetramer, hexamer, and trimer.

dissociation by a trimer, also seems an unlikely pathway. First, the pathway has a significant barrier since breaking a trimer bridge bond requires almost +20 kcal/mol for DMAH and significantly more for the amide and alkoxide bridges.<sup>17</sup> Additionally, if such a pathway were valid, it would be difficult to explain the widely different rates of equilibration observed, since they do not correlate with trimer bridge strengths.<sup>18</sup> On the basis of experimental observations (with amide compounds) showing that larger terminal alkyl groups cause slower equilibration, it was suggested the attack step could be rate limiting.<sup>12</sup> Larger terminal alkyl groups are expected to lessen trimer bridge strengths and ring-opening steps should be more facile. For DMAH, formation of an open ring is endothermic by ~20 kcal/mol, and the overall reaction 3 is endothermic by only ~24 kcal/mol, so that self-attack should occur without a significant barrier. To be rate limiting, the self-attack step would have to exhibit an anomalous low preexponential, which seems unlikely. Another argument against the second mechanism is that the equilibrium of the above pathway (eq 3) lies strongly towards the trimer, so that the forward reaction is unfavorable. However, considering the slow equilibration rates observed experimentally, the later argument might not totally discount the mechanism.

A third reaction pathway comprises ring opening of dimers or trimers and attack on another dimer or trimer. These types of reactions could provide a direct link between dimers and trimers by involving monomers, as shown below [eqs 4a and 4b], but it is thermodynamically more favorable to form higher oligomers such as tetramers, pentamers, hexamers, and possibly larger units (eq 5).



Such arguments are consistent with both experimental studies, including mass spectroscopy data, and the ab initio/DFT calculations of the present study.<sup>14,19</sup> However, there are also problems with this mechanism. Taken literally, a ring opening and attack on a neighbor would be a two-step process requiring

a unimolecular ring opening of the attacking molecule and a high activation barrier (~20 kcal/mol per bridge for DMAH). Such a mechanism could not explain the trends among the different rates of equilibration for aluminum organometallic compounds. Therefore, in the present study the favored “ring opening and attack on a neighbor” mechanism is modified to embody a concerted bimolecular reaction rather than a true “ring opening”. As shall be demonstrated, such a mechanism is consistent with most experimental observations and can account for the subtle differences observed for the various types of bridge bonding and terminal ligand arrangements.

The reaction pathways investigated for the DMAH equilibrium are illustrated in Figure 1. The mechanism involves formation of tetramer and hexamer intermediates. These oligomers allow interconversion of dimers and trimers without requiring monomers or other unstable intermediates. As implied above, reactions involving monomers are thought to be unlikely at the low temperatures where the equilibration reactions of interest occur. However, these reactions are included for completeness. Noticeably absent from the mechanism (Figure 1) are pentamers. Although it seems reasonable that pentamers should form if hexamers do, pentamers are ignored because they do not lead to a net dimer–trimer interconversion, and calculations show that these higher oligomers are present only at low concentrations as reaction intermediates.<sup>20</sup> Therefore, it is reasoned that inclusion of pentamers is not essential to understand the approach to equilibrium. Studies primarily interested in understanding liquid properties, such as viscosity, may have to consider pentamers because free energy considerations would most likely favor pentamers over hexamers. Note that fragments assigned to pentamers were observed in previous mass spectroscopy studies of DMAH.<sup>19</sup>

For the present ab initio/density functional theory (DFT) investigations of the chemical mechanisms and kinetics of the DMAH vapor phase system, alane ( $\text{AlH}_3$ ) is employed as a model system. Alane is the simplest analogue to aluminum organometallics, and a natural place to begin investigations into the vapor phase chemistry of these types of compounds. Alane serves as a model not only for DMAH, but also for other

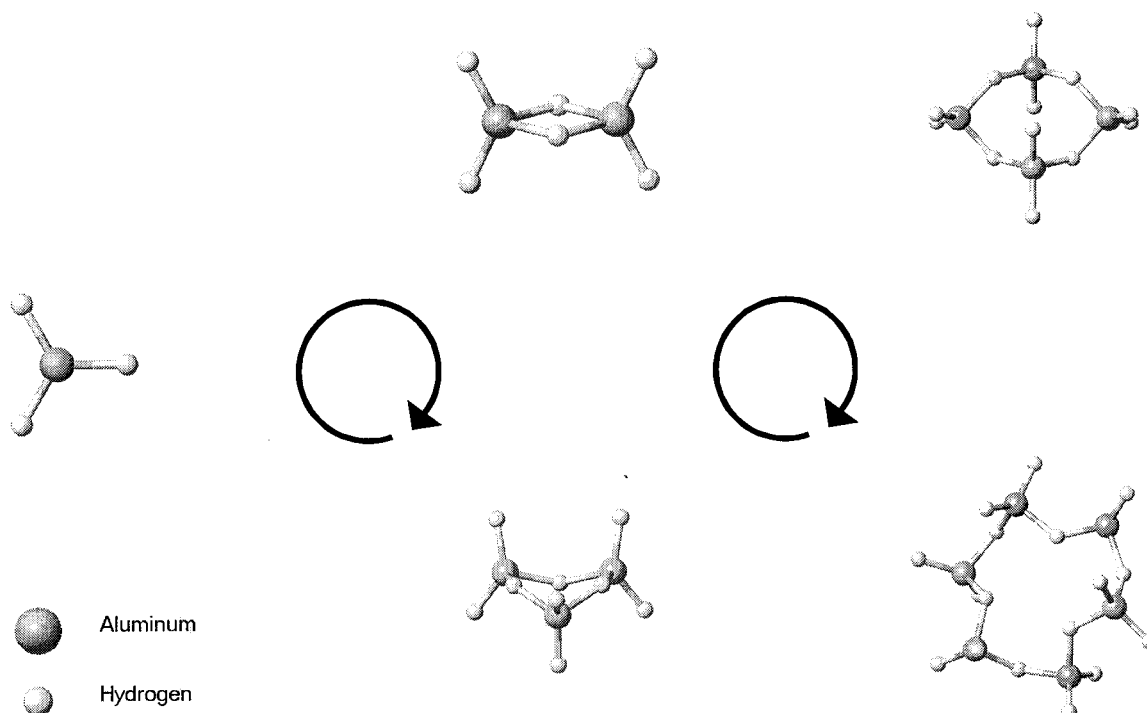


**Figure 2.** Alane reaction pathways, as a model for dimethylaluminum hydride (DMAH). Clockwise from left: monomer, dimer, tetramer, hexamer, and trimer.

**TABLE 1: Heats of Reaction ( $\Delta H^{298.15}$ ) for Dimethylaluminum Hydride (DMAH) and Alane Gas-Phase Association Reactions (Values in kcal/mol)<sup>a</sup>**

	DMAH		alane	$\Delta$
	MP2/6-31G(d,p)	B3LYP/6-31G(d,p)		
dimer $\rightleftharpoons$ 2 monomer	33.2	28.0	33.0	0.2
trimer $\rightleftharpoons$ monomer + dimer	24.2	20.0	21.5	2.7
tetramer $\rightleftharpoons$ 2 dimer	9.2	7.6	7.7	1.5
hexamer $\rightleftharpoons$ dimer + tetramer	10.8	2.7	2.8	0.1
hexamer $\rightleftharpoons$ 2 trimer	5.0	-1.6	-0.1	1.5

<sup>a</sup> Differences between DMAH and alane heats of reaction for the same corresponding reactions are given in the last column. For calculations not involving a hexamer, the alane values and the differences ( $\Delta$ 's) refer to MP2 calculations. For calculations involving a hexamer, DFT values are used. Note the underbinding of DFT methods when compared to the MP2(Full) calculations.

aluminum compounds such as precursors for AlGaAs and AlN deposition.<sup>21,1</sup> Results will show that although a strict comparison of alane with DMAH may be inexact, the investigations reveal reaction pathways that shed new light on how these compounds interact in the liquid and vapor phase.

The replacement of the terminal methyl ligands in DMAH with hydrogen to form alane presents a considerable simplification for the electronic structure calculations and makes quantum chemistry calculations practical for studying the gas-phase system. However, besides the efficiency considerations of this replacement, there is support for the substitution based on comparisons of thermodynamic calculations on the two systems, DMAH and alane. For each reaction represented in Figure 1, there is an analogous one for alane involving alane monomers, dimers, trimers, tetramers, and hexamers. Figure 2 illustrates these corresponding reaction pathways for the alane system. Table 1 lists ab initio and DFT calculated heats of reaction for both DMAH and alane reaction pathways. Comparison between the two systems reveals similar heats of reaction for corresponding reaction steps. The largest difference of  $\sim 2.7$  kcal/

mol for the trimer  $\rightarrow$  monomer + dimer reaction is relatively small compared with the overall heat of reaction. These similarities in computed thermodynamics for the reaction cycles provide support for using alane as a model system. It is an assumption of the present investigation that these similarities also exist for calculations of activation energies and reaction rate constants, at least semiquantitatively.

## II. Theoretical Methods

Optimized structures and transition-state geometries were computed using the Gaussian 94 suite of programs.<sup>22</sup> Frequency calculations were performed with analytic gradient techniques to provide zero-point energies and for calculation of thermal energy corrections. Statistical mechanical relations were used to compute entropies and Gibbs free energies for the calculation of equilibrium constants. Equilibrium predictions were accomplished using temperature-dependent equilibrium constants and the ideal gas approximation.<sup>23</sup>

Transition states were optimized using the synchronous transit-guided quasi-Newton QST methods to attain approximate transition-state structures.<sup>24,25</sup> Analytic force constants were calculated for the QST structures, and the Berny saddle point algorithm was used to subsequently optimize the structures.<sup>26,27</sup> For reactions involving hexamers, considerable difficulty was encountered in both geometry optimizations and transition-state optimizations. The apparently flat potential energy surface required numerous iterations to find a minimum, because while forces remained small, large displacements continued. Optimizations were considered complete when the forces became vanishingly small.

Calculations were performed using primarily density functional methods with some additions of MP2(full) single-point energy calculations. For investigations involving DMAH, DFT calculations refer to the B3LYP functional.<sup>28-30</sup> During the course of study, it was found that the B3PW91 functional more accurately describes bridge bonding in these aluminum com-

pounds.<sup>17</sup> Therefore, calculations involving the reaction pathways of alane utilized the B3PW91 functional.<sup>31</sup> Transition-state calculations involving the large hexamer-like structures employed a 3-21G\* basis set. The 3-21G\* and 3-21G\*\* basis sets were previously found to provide reasonable accuracy for these types of aluminum organometallic systems.<sup>32</sup> The small 3-21G\* basis set was used for efficiency because of the need to calculate force constants analytically. Unfortunately, the difficult nature of the potential energy surface made it unrealistic to simply reoptimize transition-state structures at higher basis set levels. For saddle point optimizations involving dimeric and tetrameric structures and for all geometry optimizations, a larger 6-31G(d,p) basis set was used.

Previous studies have shown that DFT methods may not properly compute the thermodynamics of bridge bonded structures such as these aluminum organometallics.<sup>17</sup> Whether the problems with calculating heats of reaction will extend to calculating activation energies is yet unknown. However, given the errors in heats of reaction, at least one of either the forward or reverse activation barriers may be in error. MP2(full)/6-31G-(d,p) calculations are included in this study to briefly explore this issue, but the size of the molecules prohibits extensive investigation of the differences between ab initio and DFT predictions. Instead, DFT methods are relied upon to produce at least a semiquantitative account of the chemical mechanisms. A rigorous comparison between ab initio and DFT predictions of activation barriers for reactions of bridge-bonded compounds remains an area for future investigation.

### III. Results

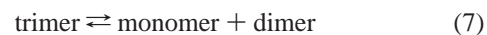
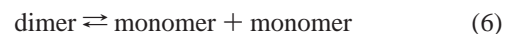
**Structures.** Previous studies have shown that density functional theory methods are reliable for predicting geometric structures of bridge-bonded aluminum compounds.<sup>17</sup> Therefore, only a brief account of the alane and DMAH structures is given here, to aid in visualization of the reactions. Figures 1 and 2 illustrate optimized structures for the monomer, dimer, trimer, tetramer, and hexamer of DMAH and alane, respectively. Skeletal structures of monomeric and dimeric DMAH and alane are similar, but monomers have  $D_{3h}$  symmetry for alane and  $C_{2h}$  symmetry for DMAH. Both alane and DMAH dimers have  $D_{2h}$  symmetry. Calculations predict that while DMAH trimers and tetramers prefer a planar arrangement with high symmetry ( $D_{3h}$  and  $D_{4h}$ ), alane adopts pseudotetrahedral Al–H bonds and a lower overall symmetry. The planarity of DMAH rings is somewhat of an irregularity among these types of aluminum organometallics. For other planar trimers, such as the *tert*-butyl amide trimer, steric arguments have been employed to explain the anomaly.<sup>21</sup> The observation that DMAH trimers and tetramers are planar suggests electronic effects may also be important. (Terminal methyl ligands would not appear to have strong steric interactions, unless the ring is abnormally small compared to other trimers.) The alane trimer adopts a boat configuration with  $C_s$  symmetry, and the tetramer takes on a  $C_{2h}$  structure. The  $C_{2h}$  tetramer is significantly different from a previously reported structure with  $C_{2v}$  symmetry.<sup>33</sup> In the previous work, an energy difference of  $\sim 1$  kcal/mol was noted between the more stable  $C_{2v}$  structure and the planar  $D_{4h}$  structure of the alane tetramer. For the present  $C_{2h}$  structure, the energy difference is closer to 3 kcal/mol, indicating the  $C_{2h}$  isomer may be more stable than the  $C_{2v}$  form. Al–H–Al ring bond angles of the  $C_{2v}$  structure from the above reference are reported near linear, whereas the present  $C_{2h}$  structure has angles close to  $130^\circ$ . These rather large differences may be due to the use of the SCF (Hartree–Fock) optimization in the previous

work, whereas the present studies include electron correlation effects in geometry optimizations (DFT methods). For calculation of the reaction energy of tetramer  $\rightleftharpoons 2$  dimers, where electron correlation was included in the previous work, their value of +8.0 kcal/mol agrees fairly well with the present results. As it has not been published previously, a vibrational spectra for the DMAH tetramer is provided in the appendix. These vibrational assignments may prove useful for identifying the tetramer in experimental studies.

Hexamers of both alane and DMAH have complex, distorted ring structures. The DMAH hexamer adopts a nonplanar contorted ring with terminal methyl groups projecting out of the ring, and pseudotetrahedral environments of bridging hydrogen atoms around each aluminum atom (Figure 3a). Although not constrained by symmetry in the optimization, the minimized structure appears to have at least a  $C_2$  symmetry axis. Apparently, the angle strain of a planar  $D_{6h}$  structure is prohibitive for DMAH. The difference in energy between the  $D_{6h}$  and  $C_2$  structure is small, however, approximately 1.5 kcal/mol calculated with the B3LYP/6-31G(d,p) method.<sup>34</sup> Due to the absence of imposed symmetry in the calculation, the DMAH hexamer bond angles vary around the ring with values of  $\sim 93^\circ$  for H–Al–H, two each of  $159^\circ$ ,  $146^\circ$ , and  $177^\circ$  for Al–H–Al bond angles, and  $\sim 126$ – $127^\circ$  for terminal C–Al–C angles. Bond lengths are approximately 1.69–1.70 Å for Al–H<sub>bridge</sub> bonds, and  $\sim 1.97$  Å for Al–C<sub>terminal</sub> bonds. Al–Al distances vary around the ring with two each of 3.33, 3.25, and 3.37 Å. The double degeneracy of the Al–H–Al angles and Al–Al distances reflect the implied  $C_2$  axis of the hexamer. A higher molecular symmetry might be obtained by imposing symmetry on the Al–H–Al angles and Al–Al distances, but unfortunately, verifying that a higher symmetry structure was indeed a true minimum (via a frequency calculation) is not practical given our current resources.

The optimized alane hexamer in the present study has no apparent symmetry ( $C_1$ ) (Figure 3b). However, calculations indicate the hexamer traverses a rather flat PES, so that many conformations may be nearly equivalent. One way to visualize the alane hexamer is to consider six AlH<sub>2</sub> groups, arranged in a ring with bridging hydrogen atoms and pseudotetrahedral environments. Another approach is to imagine a ring formed from three dimers, each with a terminal hydrogen ligand acting as a bridge to another dimer on one end, and accepting a terminal hydrogen bridge from another dimer on the other end. The first approach provides a closer parallel to the DMAH hexamer, but the second underscores an ambiguity as to the labeling of terminal and bridging hydrogen atoms in the alane hexamer.

**Monomer Reaction Pathways.** Equilibrium calculations indicate that monomers are essentially nonexistent at low to moderate temperatures, because DMAH is bound as higher units such as dimers and trimers.<sup>20</sup> However, for completeness, two reactions involving monomers are included in the gas phase model. Although these reactions are not expected to be important for the DMAH system (see introduction), these reactions could have importance to other systems where monomers are initially bound as adducts and subsequently react to form dimers, trimers, etc. The reactions considered are



In the above reaction scheme, dimers and trimers decompose via unimolecular reactions and free monomers may then react with other molecules to form dimers, trimers and possibly higher



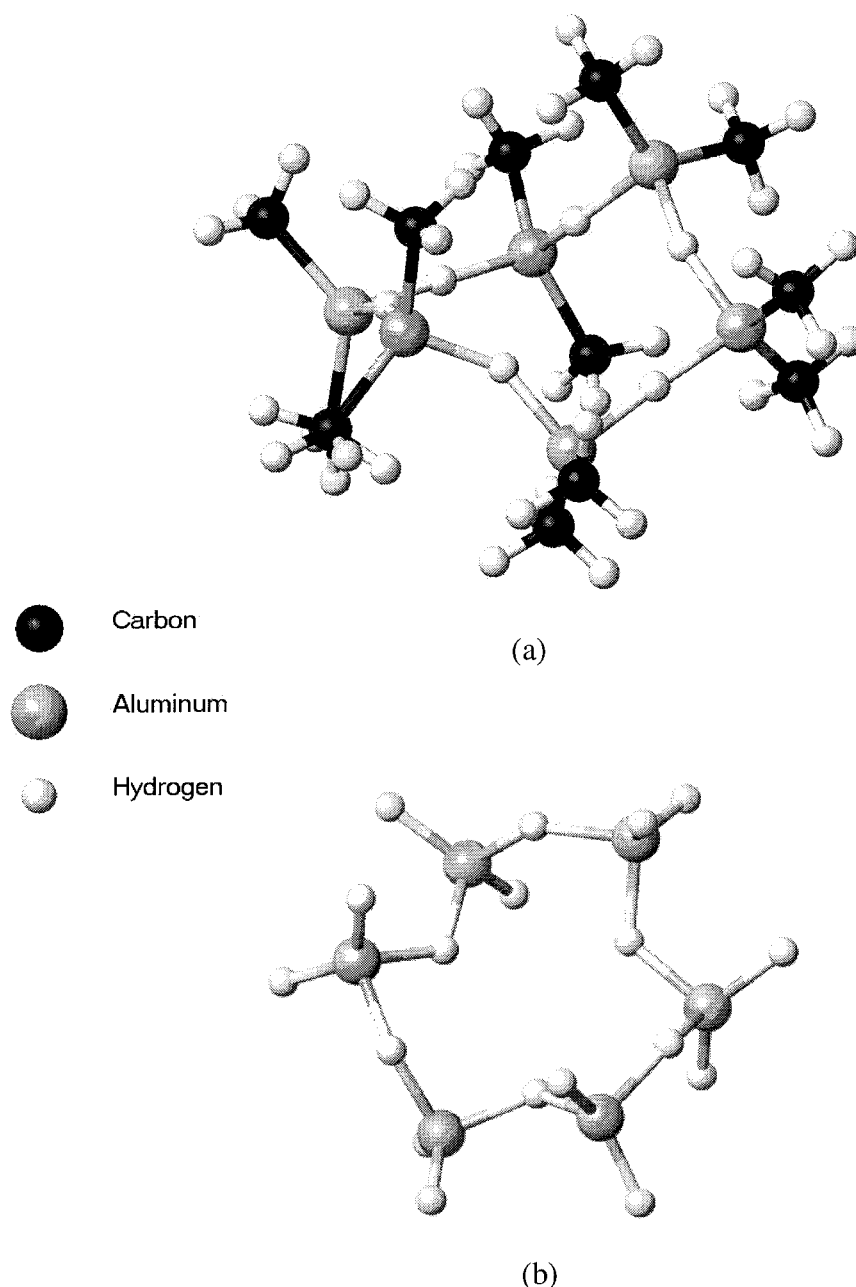


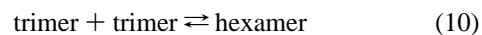
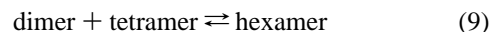
**Figure 3.** (a) Optimized DMAH hexamer. (b) Optimized alane hexamer.

order units. In this way, a contribution to the dimer  $\rightleftharpoons$  trimer interconversion could possibly occur. Other reactions involving monomers, such as tetramer  $\rightleftharpoons$  monomer + trimer, pentamer  $\rightleftharpoons$  monomer + tetramer, and hexamer  $\rightleftharpoons$  monomer + pentamer are also conceivable (through ring opening and self-dissociation), but are not considered to be important.

DFT calculations find that neither of the above reactions (eqs 6 and 7) has a classical transition state. Figure 4 plots the potential energy of a DMAH dimer as it is stretched to form two monomers. The reaction path is purely endothermic with a large barrier, corresponding to the heat of dissociation. Note the plot was generated with DFT methods that underpredict binding strengths of bridge-bonded compounds.<sup>17</sup> The actual barrier for dissociating the DMAH dimer is near +35 kcal/mol. Investigations find that dissociation of trimer into monomer and dimer also shows no classical transition state, and the activation barrier is the heat of reaction, close to +24 kcal/mol.

**Dimer, Trimer, Tetramer, and Hexamer Reaction Pathways.** Reactions among dimers, trimers, tetramers, and hexamers

were explored employing alane as a model system. The reactions of interest are



These reactions provide a pathway between dimers and trimers which involves only stable intermediates rather than the reactive and (virtually nonexistent) monomer. In this scheme (Figures 1 and 2), dimers react via an exothermic reaction (Table 1) to form energetically stable tetramers. Tetramers further react with dimers in another exothermic reaction to form hexamers. Hexamers subsequently decompose into either trimers or back to dimers and tetramers. In the opposite direction, trimers combine in a mildly exothermic reaction (ab initio MP2 values are favored) to form hexamers that then may decompose to dimers and tetramers. Tetramers further decompose to dimers.

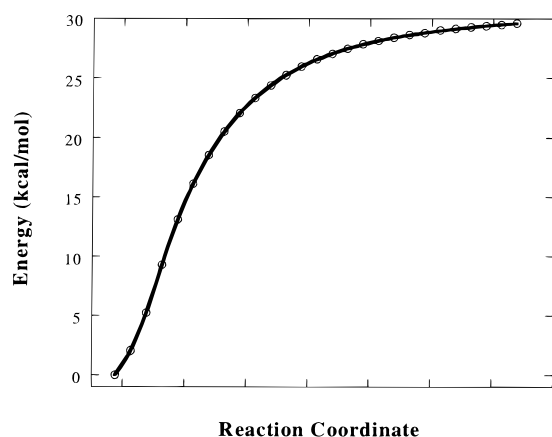


**Figure 4.** Potential energy vs reaction coordinate for the (DMAH) reaction  $\text{dimer} \rightleftharpoons 2 \text{ monomer}$ , from density functional theory calculations. There is no apparent activation energy for the reverse, recombination reaction. The reaction coordinate is defined here as the aluminum–aluminum distance as the dimer is stretched into 2 monomers.

**TABLE 2: DMAH Binding Energies (298.15 K) Per Bridge for Each Oligomer (Values in kcal/mol)<sup>a</sup>**

	B3LYP	MP2
monomer	0.0	0.0
dimer	14.0	16.6
trimer	16.0	19.1
tetramer	15.9	18.9
hexamer	15.7	19.9

<sup>a</sup> A 6-31G(d,p) basis set was used for both DFT and ab initio calculations.

Ultimately, this reaction pathway results in equilibrium between dimers and trimers. Table 2 lists bridge binding strengths of each oligomer. As is apparent from the table, enthalpic considerations favor higher oligomers, while it is clear (for gas phase calculations) that entropic considerations favor smaller units. The calculations indicate the hexamer has the strongest bridge bonds. Both experiments and calculations observe that in the vapor at room temperature trimers are apparently the best compromise, with the lowest free energy.<sup>20</sup> Higher temperatures shift the balance in favor of dimers. A condensed phase could favor the larger oligomers: tetramers, pentamers, hexamers, and possibly larger units.

A transition state was located for the concerted reaction between two dimers to form a tetramer (eq 8). The reaction occurs via a “side-on” collision of two dimers, in which bridging hydrogen atoms are conserved (see later discussion). An illustration of the transition-state geometry is shown in Figure 5. The transition-state complex is skewed away from planar, and involves two five-coordinate-like aluminum atoms. Given the relatively small size of the molecules in this reaction (16 atoms), a comparison between the ab initio (MP2) and DFT predicted activation barriers was performed, at a reasonable basis set level. A schematic of the potential energy versus reaction coordinate is shown in Figure 6. As anticipated, the reverse reaction barriers are significantly different ( $> 3$  kcal/mol) for ab initio and DFT predictions. DFT and MP2 calculated reverse activation barriers are 13.9 and 17.5 kcal/mol, respectively. Fortunately, forward activation barriers are in good agreement at 8.7 and 9.5 kcal/mol for the DFT and MP2 methods, respectively. The poor agreement for the reverse reaction barrier is consistent with DFT errors in calculations of heats of reaction.<sup>17</sup> It is apparent that an accurate description of bridge bonding is more crucial for the reverse reaction. These results suggest that for the  $2 \text{ dimer} \rightleftharpoons \text{tetramer}$  reaction, the transition-

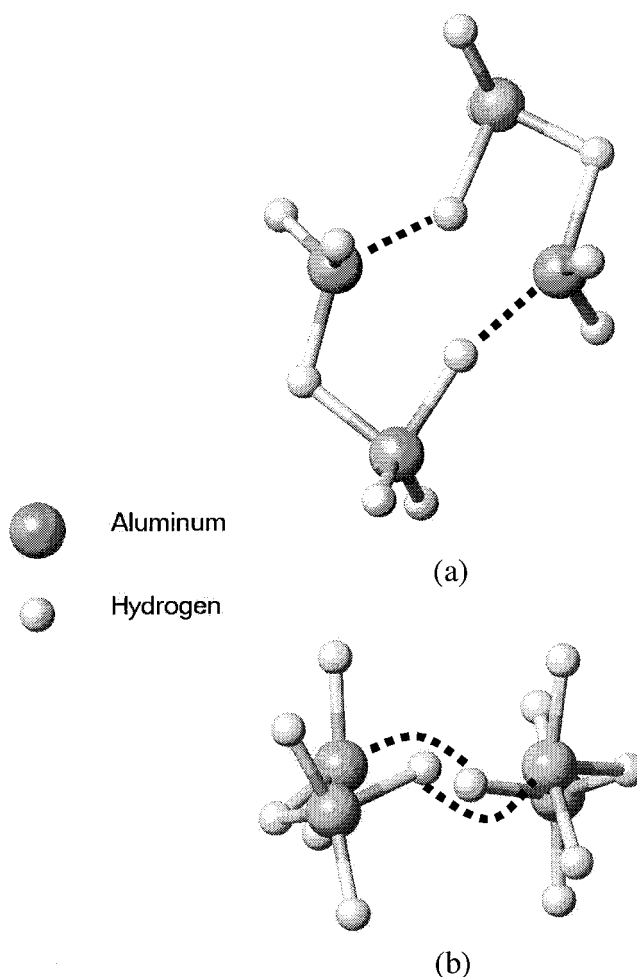


**Figure 5.** Transition state for alane reaction  $2 \text{ dimer} \rightleftharpoons \text{tetramer}$ . (a) Top view. (b) Side view. Newly forming bonds en route to a tetramer are indicated with dashed lines.

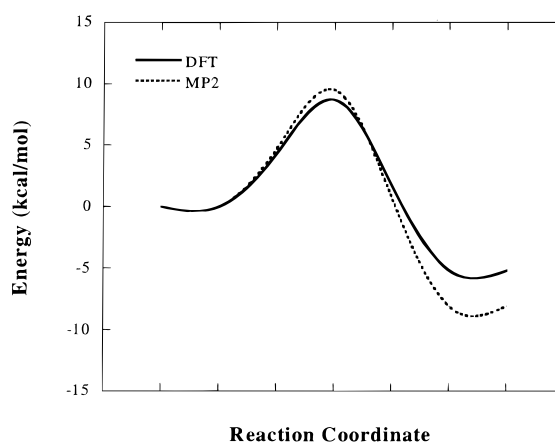


**Figure 6.** Potential Energy Surface ( $\Delta E^{\text{0K}}$ ) for the alane reaction  $2 \text{ dimer} \rightleftharpoons \text{tetramer}$ . Both DFT and MP2 calculations are represented.

state bonding is not too different from normal bonding arrangements so that DFT methods are successful at predicting the forward barrier.

Reactions involving formation of alane hexamers are found to exhibit an associative complex between reactants (dimer + tetramer, and trimer + trimer) (Figures 7 and 8). Transition states for the reactions (eqs 9 and 10) occur between the associated complexes and the hexamer product. For the dimer + tetramer reaction, DFT calculations predict that the associated complex is bound with respect to the reactants by 1–2 kcal/

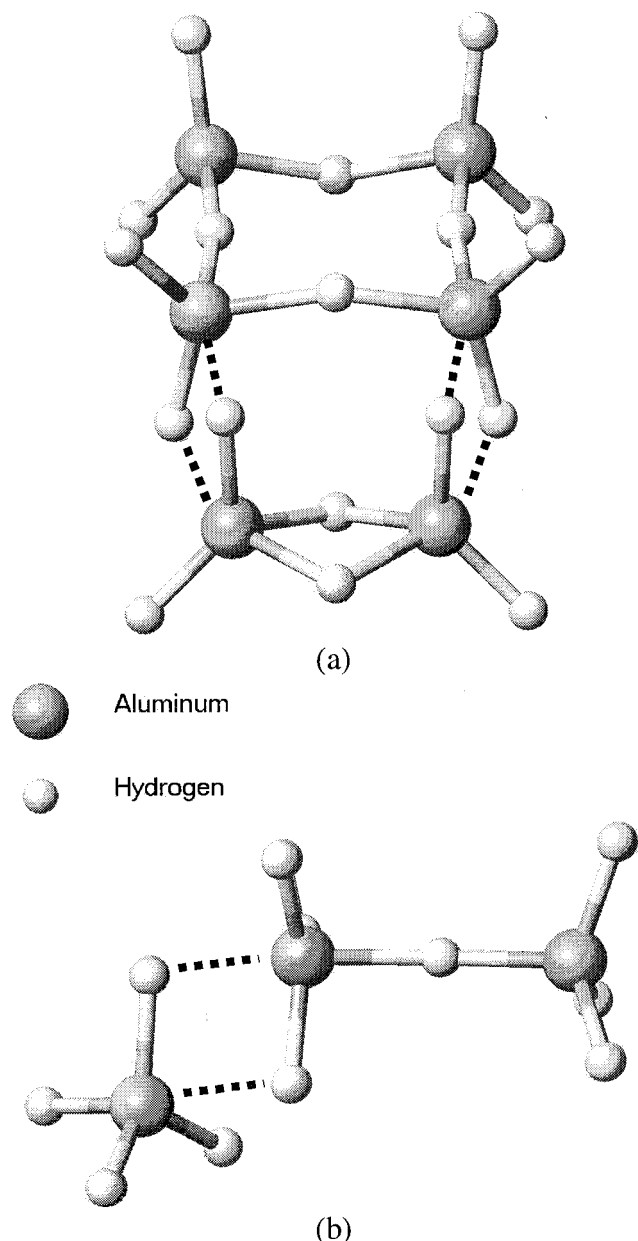


**Figure 7.** Alane dimer-tetramer associated complex. (a) Top view. (b) Side view. In the parts a and b, the dimer is shown on the bottom and left of the picture, respectively. Dashed lines indicate the attractive aluminum–hydrogen interactions that form the complex.

mol. Interestingly, MP2 calculations predict no dimer + tetramer-associated complex. In the case of trimers, the associated complex is more strongly bound, approximately 4–5 kcal/mol with DFT methods and 3–4 kcal/mol by MP2 methods ( $\Delta E^{\text{0K}}$ ).

The transition state for the pathway between the associated dimer–tetramer complex and the hexamer is illustrated in Figure 9. In the associated complex, terminal hydrogen atoms of the dimer are attracted to aluminum atoms in the tetramer, forming a five-coordinate-like structure. Terminal hydrogen atoms of the tetramer are likewise attracted to the aluminum atoms of the dimer. The reaction proceeds through a partial interchange of bridge and terminal hydrogen atoms. Because of the complex nature of the bonding in the alane hexamer, it is not convenient to strictly label bridge and terminal bonds, but it is clear that bridge and terminal characteristics are interchanged in the transition state. From the associated complex, the dimer-tetramer

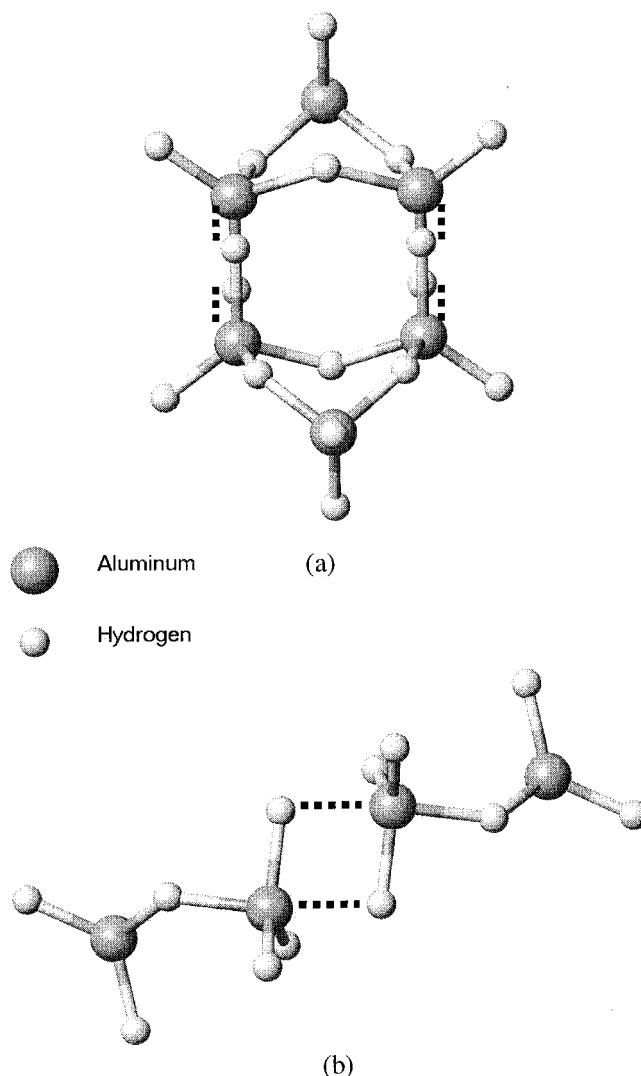


**Figure 8.** Alane trimer-trimer associated complex. (a) Top view. (b) Side view. Dashed lines indicate the attractive aluminum–hydrogen interactions that form the complex.

unit surmounts a  $\sim 7.7$  kcal/mol activation energy barrier (DFT) to form a hexamer. MP2 calculations do not manifest an associated complex, but predict a similar activation barrier of 7.3 kcal/mol. Reverse activation barriers are calculated as 10.7 and 14.4 kcal/mol for DFT and MP2 methods, respectively. Again it appears that DFT methods perform well for the forward barrier, but are in error for the reverse, dissociation reaction. A schematic of the potential energy surface for the dimer + tetramer  $\rightleftharpoons$  hexamer reaction is shown in Figure 10.

Verification that the transition state corresponds to the reaction of interest was accomplished by displacing the transition-state complex on either side of the barrier and allowing the structure to minimize. Displacing the transition state toward the reactant (associated dimer + tetramer) clearly converged to the associated complex. Following the other side of the transition state downhill toward the products realized a linear form of the alane hexamer (Figure 11). B3PW91/3-21G\* calculations find the linear isomer is more stable than the cyclic form by  $\sim 3$  kcal/mol. To test whether results are an artifact of the small basis set (3-21G\*) used in the minimization, the optimized linear and cyclic forms were compared with a single point B3PW91/6-31G(d,p) calculation. The larger basis set did not change the order of stability. It is reasoned, therefore, that the transition state is identified with the dimer + tetramer  $\rightleftharpoons$  hexamer reaction;

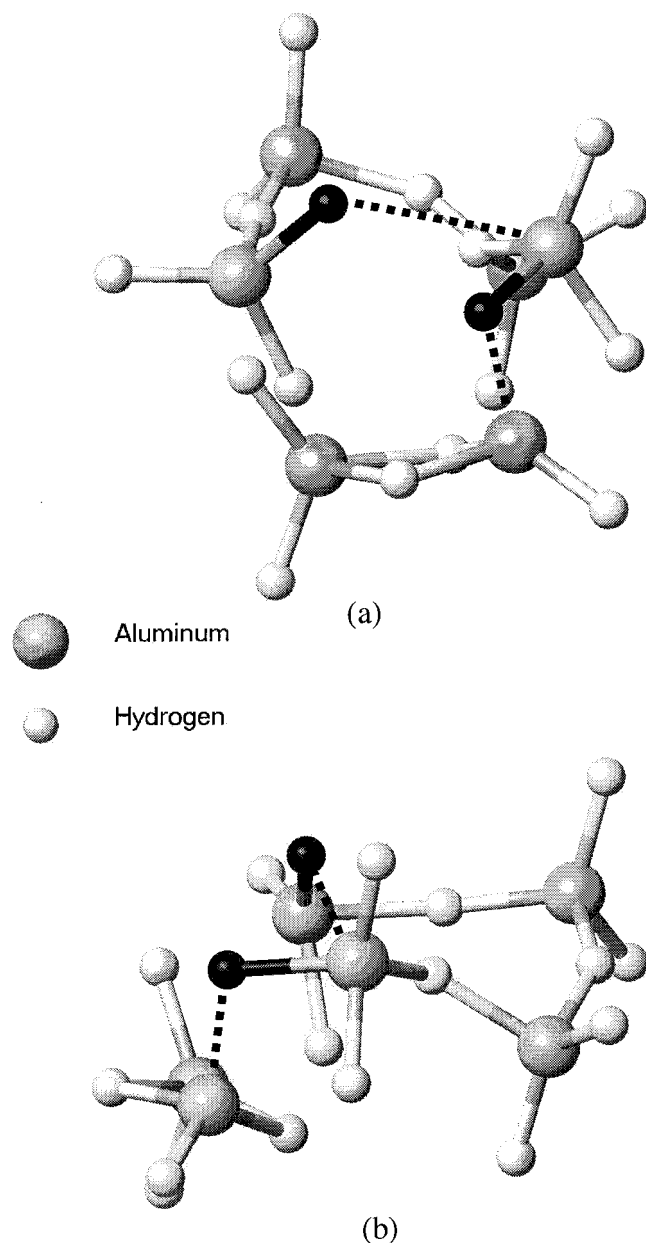


**Figure 9.** Optimized transition-state structure for the alane reaction dimer + tetramer  $\rightleftharpoons$  hexamer. Two representative hydrogen atoms that interchange bridge-terminal roles are darkened. Dashed lines indicate breaking bonds of the dimer and tetramer en route to forming a hexamer. In parts a and b, the reactant dimer is located at the bottom and left side of the activated complex illustration, respectively. It may be inferred from the pictures that the distinction between bridge and terminal-type bonds is ambiguous.

however, the product side of the transition state exhibits a relatively flat PES where both linear and cyclic isomers are possible products. Simply following the transition state downhill via an optimization results in the lowest energy conformer, the linear hexamer. The unbound state of the cyclic hexamer with respect to the linear form is apparently an indication that alane as a model for DMAH breaks down. The equivalence of terminal and bridge ligands in the alane structure allows it to form chains and still retain most of the stability of the hydrogen bridges, while relieving ring strain. DMAH, on the other hand, is expected to prefer the cyclic structure, as this arrangement maximizes the number of hydrogen bridge bonds. Substituting hydrogen bridge bonds with methyl bridges to form a linear DMAH hexamer would be energetically unfavorable. Consider-

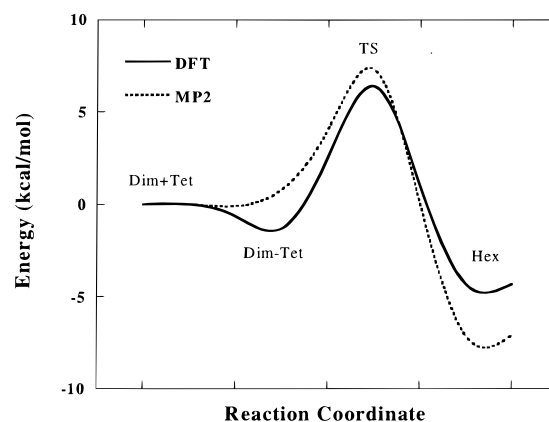


**Figure 10.** Potential energy surface ( $\Delta E^{\text{0K}}$ ) of the alane reaction dimer + tetramer  $\rightleftharpoons$  hexamer. In the figure, Dim = dimer, Tet = tetramer, Dim-Tet = dimer + tetramer complex, TS = transition state, and Hex = hexamer.

ing that unconstrained geometry optimizations of the cyclic alane hexamer were successful, there must be at least a small barrier to dissociation of the cyclic hexamer into the linear isomer. Unfortunately, searches along the intrinsic reaction coordinate, to locate the reaction product more exactly, are not currently practical.

The 2 trimers  $\rightleftharpoons$  hexamer reaction is similar to the above dimer + tetramer reaction. Hexamer formation from the associated trimer complex again involves bridge-terminal exchange. For this reaction, however, a single transition state between the associated trimer complex and the hexamer could not be located. Part of the difficulty is that the endothermic nature of the reaction, as predicted with DFT methods, suggests the transition state may lie close to the hexamer. Because of the many ring modes of the contorted alane hexamer, it is difficult to characterize that portion of the potential energy surface. Alternatively, there may not exist a single transition state that separates the reactants and products. Potential energy surface searches found two similar “intermediate” transition-state configurations involving the successive opening of each trimer ring. These observations indicate the reaction could occur through rapid sequential opening of trimer rings. From these potential energy searches, it appears reasonable that the ring openings occur through a bridge-terminal exchange similar to the dimer + tetramer reaction. From point-by-point exploration of the potential energy surface along the expected (constrained) reaction pathway, an activation barrier near  $\sim 8$  kcal/mol (from the associated complex) is estimated. This barrier is consistent with the 2 dimer  $\rightleftharpoons$  tetramer and dimer + tetramer  $\rightleftharpoons$  hexamer reactions.

#### IV. Discussion

**Reaction Pathways.** The concerted reaction pathways presented in the previous sections present plausible alternatives to reaction mechanisms requiring ring opening and bridge-bond breaking. Bimolecular activation barriers are substantially less than bridge bond dissociation energies, and barriers for the reverse unimolecular reactions are also less than for ring-opening steps.

In the reaction 2 dimers  $\rightleftharpoons$  tetramer, the  $\sim +9$  kcal/mol barrier is nearly half the cost of breaking a 17.5 kcal/mol dimer bridge bond. Therefore, a bimolecular “side-on” attack is a probable reaction pathway for formation of tetramers. In this reaction, the “side-on” collision retains the identity of the bridge bonds, and terminal groups are relatively inert to the reaction.



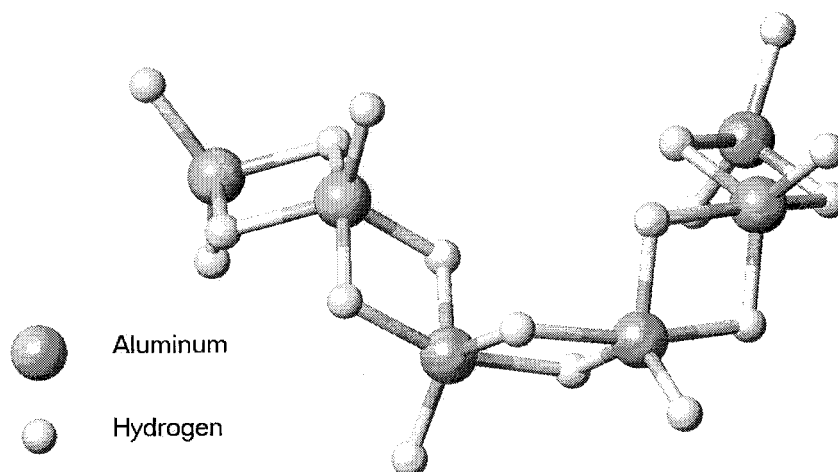


**Figure 11.** Optimized linear alane hexamer. Note the ambiguous assignment of bridge and terminal-type bonds in this polymeric-like structure.

The analogy between alane and DMAH is relatively straightforward, and both the mechanism and activation barrier may be well described with the alane model. For this 2 dimers  $\rightleftharpoons$  tetramer reaction only, the transition state for the actual DMAH reaction was also obtained. The reaction follows a similar pathway to the alane reaction, with substitution of methyl groups at the terminal positions. Electronic energy calculations by DFT methods predict a forward barrier very close to that of the alane reaction (within  $\sim 1$  kcal/mol), but including zero-point energies raises the DMAH activation barrier to  $\sim 14$  kcal/mol. These results provide additional support for employing alane as a model system to explore gas-phase reactions of aluminum organometallic compounds.

The reverse reaction, unimolecular decomposition of tetramers, has a barrier near  $+18$  kcal/mol (MP2 value) which is comparable to a ring-opening step. Depending on the details of the self-dissociation pathway, a ring-opening mechanism and reclosing to exclude monomer could compete with the concerted reaction. However, unlike the concerted reaction, ring-opening reactions would be expected to have an extremely fast reverse reaction as well, since the equilibrium favors ring structures (no free monomer). Further investigations of the accuracy of the MP2 calculated unimolecular activation barrier would be in order before pursuing a ring-opening mechanism.

Reactions involving hexamers are more complicated since they introduce associated complexes between reactants, a mixed terminal-bridge-bonding arrangement in the alane hexamers, and linear hexamers. Efforts were made to locate a "side-on" collision pathway for formation of hexamers that proceeded through dimer insertion into a tetramer, or trimer insertion into another trimer. These pathways would be analogous to reaction 8 where dimers insert into one another, conserving the labeling of bridge atoms. Transition state searches for such configurations resulted in numerous imaginary modes, which upon relaxation drastically changed the look of the transition state, and the presumed reaction coordinates developed into hexamer ring vibrations. The cause for these distortions is evident in the appearance of the complex shape of the alane hexamer (Figure 3b). The simple  $D_{2h}$  and  $C_{2h}$  structures of the dimer and tetramer, respectively, require significant distortion to form the contorted hexamer. While the transition state searches could not cover every possibility, it is likely there is no single saddle point that separates the reactants and products in a fashion that occurs through a "side-on" collision of alane dimer and tetramer. Given that the DMAH hexamer is similarly contorted, while the dimer, trimer, and tetramer reactants are of high symmetry ( $D_{2h}$ ,  $D_{3h}$ ,

$D_{4h}$ ), it seems likely that transition-state optimizations involving DMAH hexamers may encounter similar difficulties. Considering the lower symmetry of the final product it is a challenge to find a single saddle point separating reactants and product in this "side-on" fashion. It may also be that DFT methods are not particularly suited for searches on the PES of these bridge-bonded compounds.

The generation of an associated complex between dimers and tetramers or trimers provides the necessary precursor to the formation of hexamers. Bridge-terminal exchange of hydrogen atoms allows a concerted reaction between the relatively symmetric  $D_{2h}$ ,  $C_s$ , and  $C_{2h}$  structures of the alane dimer, trimer, and tetramer, respectively, and the distorted zigzag form of the hexamer. From the reverse reaction point of view, forming a dimer or trimer from the hexamer can also proceed through a concerted reaction step where the ring narrows, terminal bonds fold into bridge bonds, and vice versa. These reverse reactions occur with lower activation barriers compared to alternative ring-opening pathways.

Peculiarities of the alane reaction pathways impose some uncertainty as to the applicability of alane as a model system for DMAH, but also suggest unconventional reaction pathways for these types of compounds. DMAH most likely also forms associated complexes between dimers, trimers, tetramers, and hexamers, but with weaker forces. DMAH associated complexes would be expected to be less strongly bound due to weaker methyl bridging interactions and steric constraints of the methyl groups. Such associated complexes may proceed to hexamers (and possibly higher oligomers) through similar concerted reaction steps in which terminal methyl groups exchange with bridging hydrogen atoms, temporarily. Methyl bridges are significantly weaker than hydrogen bridges ( $\sim 10$  kcal/mol per methyl bridge vs  $\sim 19$  kcal/mol per hydrogen bridge), but once a hexamer is formed, a rapid intramolecular bridge-terminal exchange produces the thermodynamically more stable hydrogen bridged structure. Bridge-terminal exchange reactions are known to occur rapidly in these types of compounds. For trimethyl-aluminum (TMA), it is necessary to go to low temperatures ( $-75$  °C) to resolve bridge and terminal signals in NMR experiments.<sup>19</sup> This proposed methyl-bridge-mediated kinetic pathway may be an alternative to a direct insertion or ring-opening mechanism. Such a concerted mechanism could also operate for other dimer  $\rightleftharpoons$  trimer systems such as the organo-aluminum amide compounds.<sup>21</sup> For these compounds, the relatively stronger nitrogen bridge bonds make it even more likely a concerted mechanism is operative.

The preference of alane for the linear hexamer represents a deficiency of alane as a model for DMAH, but is not expected to invalidate the semiquantitative picture formed from the alane system. Starting from the tetramer–dimer complex, the forward activation barrier should not be affected by the presence of the linear hexamer on the other side of the barrier. The alane linear hexamer owes its stability to the equivalence of terminal and bridge ligands. DMAH would not be expected to exhibit a linear hexamer due to the energetic dissimilarity of hydrogen and methyl bridges. A downhill search from a DMAH transition state to the hexamer product would be expected to arrive at the optimized cyclic hexamer.

From these studies, several observations can be made regarding the complex liquid and vapor phase reactions of DMAH. Calculating half-lives of both the forward and reverse reaction for 2 dimers  $\rightleftharpoons$  tetramer sheds some light on the experimentally observed behavior of DMAH. Using standard formulas for first and second-order reaction half-lives and a concentration of  $1.1 \times 10^{-4}$  mol/L ( $\sim 2$  torr, the vapor pressure of DMAH) gives values of  $t_{1/2} \approx 13.6$  min, and 66 s for the forward and reverse reactions, respectively, at 298 K. These calculations suggest the vapor phase equilibrium proceeds through a series of slow bimolecular reactions and relatively faster unimolecular reactions. The sequence of these reaction steps between dimers and trimers results in slow kinetics to reach equilibrium.

The prediction of associated complexes between dimers, tetramers, and trimers also provides some insight into DMAH liquid properties. If the gas-phase results are qualitatively transferable to the liquid, then these associated complexes may account for the observed high viscosity ( $\sim 6000$  cP) of neat liquid DMAH.<sup>35</sup> In addition, the stronger calculated interactions between trimers as compared to dimers and tetramers may explain variations in viscosity due to changes in the composition of the liquid. Perturbing the system from equilibrium, as for example by heating, is expected to result in a slow return to equilibrium, with time dependent liquid properties. Additionally, mixing additives such as amine adducts into DMAH will shift the equilibrium toward the adduct and away from the higher oligomers and the associated complexes responsible for the high viscosity.<sup>35</sup>

The presently studied reactions may also be extended to a possible pathway for the gas-phase disproportionation of DMAH. The reaction  $3 \text{DMAH}_{(g)} \rightleftharpoons 2 \text{TMA}_{(g)} + \text{AlH}_3_{(g)}$  is approximately thermoneutral, with a Gibbs free energy change of +1.4 kcal/mol (G2 values).<sup>36</sup> On the basis of the present studies, this gas-phase disproportionation reaction may proceed through formation of a tetramer (2 dimer  $\rightleftharpoons$  tetramer). Rearrangement of the tetramer through a bridge-terminal exchange and subsequent dissociation back to dimers could provide a mechanism to exchange hydrogen and methyl ligands. Repetition of these exchange reactions would result in a gas-phase disproportionation to TMA and alane. Such a reaction could be important to understanding the details of thin film growth with DMAH.<sup>20</sup>

## V. Summary

A gas-phase mechanism has been investigated for the DMAH dimer  $\rightleftharpoons$  trimer equilibrium. The equilibrium pathway is important to understand the complicated time/process dependent composition of DMAH. A reaction scheme involving units from monomers through hexamers has been considered. As a practical model for electronic structure calculations, alane was implemented to develop kinetic parameters for the reaction pathways.

**TABLE 3: Infrared Active Vibrational Modes of the DMAH Tetramer<sup>a</sup>**

wavenumber (cm <sup>-1</sup> )	symmetry	infrared relative intensity
158	E <sub>u</sub>	20
287	E <sub>u</sub>	1
554	A <sub>2u</sub>	30
561	E <sub>u</sub>	10
583	E <sub>u</sub>	130
672	A <sub>2u</sub>	20
746	E <sub>u</sub>	765
769	E <sub>u</sub>	135
820	A <sub>2u</sub>	635
1264	E <sub>u</sub>	2
1264	A <sub>2u</sub>	100
1472	A <sub>2u</sub>	1
1472	E <sub>u</sub>	<1
1478	E <sub>u</sub>	<1
2001	E <sub>u</sub>	2750
3028	A <sub>2u</sub>	30
3028	E <sub>u</sub>	10
3100	E <sub>u</sub>	60
3110	E <sub>u</sub>	50
3110	A <sub>2u</sub>	20

A reaction mechanism that involves formation of higher oligomers via concerted reaction steps has been explored. Transition states were located for reactions 2 dimers  $\rightleftharpoons$  tetramer, dimer + tetramer  $\rightleftharpoons$  hexamer, and 2 trimers  $\rightleftharpoons$  hexamer.

Results with the alane system find the formation of tetramers from dimers proceeds through a “side-on” collision with conservation of bridging H atoms. (A bridge atom on the dimer becomes a bridge atom on the tetramer). Reactions involving formation of hexamers, however, proceed through a bridge-terminal exchange reaction that does not conserve the labeling of bridge and terminal bonds. Formation of hexamers from dimers, trimers, and tetramers proceeds through the initial formation of associated reactant complexes. These reactant complexes then progress through a transition state to the hexamer product. The concerted reaction occurs through a bridge-terminal exchange mechanism. The prediction of the associated reactant complexes suggests an alternative pathway for DMAH and other bridging aluminum compounds.

**Acknowledgment.** The authors gratefully acknowledge the Semiconductor Research Corporation and National Computational Science Alliance. We also acknowledge the use of the freeware molecular drawing software, WebLab ViewerLite, Molecular Simulations Inc., San Diego, CA.

## VII. Appendix

Table 3 lists vibrational modes and relative intensities of the  $D_{4h}$  DMAH tetramer, predicted with the B3LYP/6-31G(d,p) method. Previous studies of vibrational frequency predictions of DMAH dimers and trimers suggest an average accuracy of 50 cm<sup>-1</sup>, with a tendency to overpredict high wavenumber modes and underpredict modes less than 600 cm<sup>-1</sup>.<sup>17</sup> Note the intense mode at 2001, which may help distinguish tetramers from dimers and trimers. On the basis of the frequency scaling observed in previous studies of the DMAH trimer vibrational spectra, the predicted mode at 2001 may be expected experimentally near 1880–1885 cm<sup>-1</sup>.<sup>17</sup>

## References and Notes

- (1) Bhat, R.; Koza, M. A.; Chang, C. C.; Schwarz, S. A. *J. Cryst. Growth* **1986**, 77, 7.
- (2) Zhu, N.; Cacouris, T.; Scarmozzino, R.; Osgood, R. M., Jr. *J. Vac. Sci. Technol. B* **1992**, 10, 1167.

- (3) Littau, K. A.; Mosely, R.; Zhou, S.; Zhang, H.; Guo, T. *Microelectron. Eng.* **1997**, *33*, 101.
- (4) Simons, J. *J. Phys. Chem.* **1991**, *95*, 1017.
- (5) Head-Gordon, M. *J. Phys. Chem.* **1996**, *100*, 13213.
- (6) Ziegler, T. *Chem. Rev.* **1991**, *91*, 651.
- (7) Ho, P.; Coltrin, M. E.; Binkley, J. S.; Melius, C. F. *J. Phys. Chem.* **1985**, *89*, 4647.
- (8) Wartick, T.; Schlesinger, H. I. *J. Am. Chem. Soc.* **1953**, *75*, 835.
- (9) Kondoh, E.; Ohta, T. *J. Vac. Sci. Technol. A* **1995**, *13*, 2863.
- (10) Grady, A. S.; Puntambekar, S. G.; Russell, D. K. *Spectrochim. Acta* **1991**, *47A*, 47.
- (11) Only molecular rearrangement is considered, i.e., not pyrolysis.
- (12) Sauls, F. C.; Czekaj, C. L.; Interrante, L. V. *Inorg. Chem.* **1990**, *29*, 4688.
- (13) Schauer, S. J.; Robinson, G. H. *J. Coord. Chem.* **1993**, *30*, 197.
- (14) Rogers, J. H.; Apblett, A. W.; Cleaver, W. M.; Tyler, A. N.; Barron, A. R. *J. Chem. Soc., Dalton Trans.* **1992**, 3179.
- (15) Storr, A.; Thomas, B. S. *J. Chem. Soc. A* **1971**, 3850.
- (16) Sauls, F. C.; Interrante, L. V.; Jiang, Z. *Inorg. Chem.* **1990**, *29*, 2989.
- (17) Willis, B. G.; Jensen, K. F. *J. Phys. Chem. A* **1998**, *102*, 2613.
- (18) There are amide compounds with stronger bridge bonding than DMAH but with faster equilibration rates. Additionally, larger ligands generally decrease the bridge binding energies, but have slower equilibration rates.
- (19) Tanaka, J.; Smith, S. R. *Inorg. Chem.* **1969**, *8*, 265.
- (20) Willis, B. G.; Jensen, K. F. In preparation.
- (21) Sauls, F. C.; Interrante, L. V. *Coord. Chem. Rev.* **1993**, *128*, 193.
- (22) Frisch, M. J.; Trucks, G. W.; Schlegel, H. B.; Gill, P. M. W.; Johnson, B. G.; Robb, M. A.; Cheeseman, J. R.; Keith, T. A.; Petersson, G. A.; Montgomery, J. A.; Raghavachari, K.; Al-Laham, M. A.; Zakrewski, V. G.; Ortiz, J. V.; Foresman, J. B.; Cioslowski, J.; Stefanov, B. B.; Nanayakkara, A.; Challachombe, M.; Peng, C. Y.; Ayala, P. Y.; Chen, W.; Wong, M. W.; Andres, J. L.; Replogle, E. S.; Gomperts, R.; Martin, R. L.; Fox, D. J.; Binkley, J. S.; Defrees, D. J.; Baker, J.; Stewart, J. P.; Head-Gordon, M.; Gonzalez, C.; Pople, J. A. *Gaussian 94*; Gaussian, Inc.: Pittsburgh, 1995.
- (23) Due to the size of the DMAH hexamer (60 atoms), a frequency calculation at the minimum structure was not performed. Confidence that the given structure is a true minimum is based on the likeness of the DMAH hexamer to that of alane, and also to the complete optimization without symmetry constraints. Motivated by the planar structures of the trimer and tetramer, a  $D_{6h}$  symmetry hexamer was initially investigated. However, this structure had several imaginary frequencies associated with symmetry breaking motions. Employing the calculated force constants for further optimization without symmetry produced the structure shown in Figure 3a, which was used throughout the calculations. The thermal energy required for calculation of reaction enthalpies (298.15K) in Table 1 was estimated by extrapolating the thermal energy per oligomer from monomer, dimer, trimer, and tetramer calculations. The error from this procedure is estimated to be less than 1 kcal/mol by analogy to the alane system where the thermal energies for both  $C_1$  and  $D_{6h}$  symmetry hexamer structures were available from vibrational frequency calculations. Temperature-dependent equilibrium constants were calculated based on vibrational frequency data obtained from a B3LYP/3-21G\*\* calculation of the  $D_{6h}$  symmetry hexamer. The error from this assumption is, again, expected to be on the order of 1 kcal/mol.
- (24) Peng, C.; Schlegel, H. B. *Israel J. Chem.* **1993**, *33*, 449.
- (25) Peng, C.; Ayala, P. Y.; Schlegel, H. B.; Frisch, M. J. *J. Comput. Chem.* **1995**.
- (26) Frisch, M. J.; Frisch, A.; Foresman, J. B. *Gaussian 94 User's Reference*; Gaussian, Inc.: Pittsburgh, 1996.
- (27) Schlegel, H. B. *J. Comput. Chem.* **1982**, *3*, 214.
- (28) Becke, A. D. *Phys. Rev. A* **1988**, *38*, 3098.
- (29) Lee, C.; Yang, W.; Parr, R. G. *Phys. Rev. B* **1988**, *37*, 785.
- (30) Becke, A. D. *J. Chem. Phys.* **1993**, *98*, 5648.
- (31) Perdew, J. P.; Chevary, J. A.; Vosko, S. H.; Jackson, K. A.; Pederson, M. R.; Singh, D. J.; Fiolhais, C. *Phys. Rev. B* **1992**, *46*, 6671.
- (32) Barron, A. R.; Dobbs, K. D.; Francl, M. M. *J. Am. Chem. Soc.* **1991**, *113*, 39.
- (33) Shen, M.; Liang, C.; Schaefer, H. F., III *Chem. Phys.* **1993**, *171*, 325.
- (34) For the  $C_2$  DMAH hexamer, the B3LYP/6-31G(d,p) calculation is a single-point energy calculation with the B3LYP/3-21G\*\* optimized geometry. The  $D_{6h}$  symmetry structure was minimized at the B3LYP/6-31G(d, p) level, so the actual difference (within the DFT approximation) may be slightly larger.
- (35) Yun, J.-H.; Lee, J.-H.; Park, J. W.; Rhee, S.-W. *J. Electrochem. Soc.* **1998**, *145*, L23.
- (36) Curtiss, L. A.; Raghavachari, K.; Trucks, G. W.; Pople, J. A. *J. Chem. Phys.* **1991**, *94*, 7221.